AIChE

Structure and Kinetics of Gas Hydrates from Methane/Ethane/Propane Mixtures Relevant to the Design of Natural Gas Hydrate Storage and Transport Facilities

Rajnish Kumar
Dept. of Chemical and Biological Engineering, University of British Columbia, Vancouver, BC, Canada V6T 1Z3
Steacie Institute for Molecular Sciences, National Research Council Canada, Ottawa, ON, Canada K1A 0R6

Praveen Linga
Dept. of Chemical and Biological Engineering, University of British Columbia, Vancouver, BC, Canada V6T 1Z3

Igor Moudrakovski and John A. Ripmeester
Steacie Institute for Molecular Sciences, National Research Council Canada, Ottawa, ON, Canada K1A 0R6

Peter Englezos
Dept. of Chemical and Biological Engineering, University of British Columbia, Vancouver, BC, Canada V6T 1Z3

DOI 10.1002/aic.11527
Published online June 10, 2008 in Wiley InterScience (www.interscience.wiley.com).

The kinetics of gas hydrate growth from binary CH_4/C_2H_6 and CH_4/C_3H_8 and ternary $CH_4/C_2H_6/C_3H_8$ gas mixtures were obtained by the gas uptake method in a semibatch stirred vessel at constant pressure and a temperature of 273.7 K. These data are of interest for the design of facilities for natural gas storage and transportation in the solid (hydrate) state. During hydrate formation, samples from the gas phase were taken and analyzed by gas chromatography. It was found that the molar composition of CH_4 in the vapor phase increased as hydrate crystallization progressed. The observed fractionation effect (enrichment of the hydrate phase with propane) complicates the natural gas storage process. The fractionation effect was also confirmed with molecular-level studies where hydrate from the $CH_4/C_2H_6/C_3H_8$ gas mixture was characterized by powder X-ray diffraction (PXRD), NMR, and Raman spectroscopy. The hydrate phase composition and cage occupancy of each gas were calculated with the help of information obtained by Raman spectroscopy, gas chromatography, and PXRD. The results were consistent with those obtained by NMR. The composition of the gas phase and the hydrate are found to

Correspondence concerning this article should be addressed to P. Englezos at englezos@interchange.ubc.ca.

evolve over time, suggesting that kinetic and transport factors contribute in addition to thermodynamics. © 2008 American Institute of Chemical Engineers *AIChE J,* 54: 2132–2144, 2008
Keywords: gas hydrates, kinetics, methane, ethane, propane, Raman, NMR, PXRD

Introduction

Clathrate hydrate formation from gas mixtures differs from the formation from single gases for several reasons. One of these is thermodynamics: von Stackelberg noted many years ago that some gas mixtures gave a different hydrate phase than when each component was used by itself to form hydrate.[1] Another is that there are kinetic and transport limitations, for instance, gas hydrate formers have different solubilities and diffusion constants in water. As well, a hydrate crystal formed from a single component or a gas mixture may undergo structural transitions: it is very difficult to know or measure the structure of the first solid crystals that appear upon nucleation. Subramanian et al.[2] reported structure II hydrate formation from a methane (CH_4) and ethane (C_2H_6) gas mixture at particular mixture compositions. Uchida et al.[3] showed that structure II hydrate formed first from a CH_4/C_3H_8 system and that this was followed by the formation of structure I methane hydrate. Uchida et al.[3] also showed that the hydrate phase was enriched in propane. This enrichment in one hydrate former was also observed in hydrate formation from CO_2/N_2 and CO_2/H_2 mixtures.[4] It is also noted that the observed fractionation effect was also found when the gas evolved from hydrate pellets was analyzed.[5] The pellets were synthesized with a methane/ethane/propane mixture. Kini et al.[6] monitored the cavity filling through NMR measurements for the same system using ice rather than water. Schicks et al.[7] synthesized mixed hydrates of CH_4, C_2H_6, and C_3H_8 mixture, in that study two different hydrate morphologies were reported each with different cage occupancies. The different rates at which gas molecules appear to be incorporated into the hydrate as well as the role of gas phase measurements was illustrated in more recent studies on hydrate formation from a CH_4/CO_2 mixture by Uchida et al.[8] and Park et al.[9] Svandal et al.[10,11] presented phase field simulations on hydrate formation from a CH_4/CO_2 mixture and concluded that the rate is limited by mass transport of the gas to the water phase. Structure, cage occupancy, and composition of mixed hydrates formed by the binary mixtures of CH_4/C_2H_6 and CH_4/C_3H_8 are available in the literature.[2,3,12,13] Recently, Uchida et al.[14] reported spectroscopic observations on hydrates formed from binary (C_2H_6/C_3H_8), ternary ($CH_4/C_2H_6/C_3H_8$), and quaternary ($CH_4/C_2H_6/C_3H_8$/isobutene) mixtures. They reported cage occupancies which were determined by Raman spectroscopy with support from gas chromatography.

Gas hydrate formation is an exothermic crystallization process, and is characterized by nucleation followed by crystal growth and agglomeration.[15,16] The kinetics of hydrate growth is concerned with the rate at which the hydrate phase grows after the induction time that marks the onset of hydrate crystallization (nucleation point). The induction time is easily measured in the laboratory. On the other hand, the rate of nucleation (number of hydrate crystal nuclei formed per unit time per unit volume) is an extremely difficult measurement. Most hydrate growth studies involve measuring the rate of uptake of the hydrate-forming substance coupled sometimes with determination of the particle size distribution.[17–20] The rate of hydrate crystal growth is defined operationally. One may use the gas uptake rate or the rate at which a hydrate interface advances. The question that arises is how an intrinsic rate can be distinguished from the relevant transport processes. It is not easy to answer this question and consequently, kinetic studies focusing on particular hydrate forming systems and hydrate vessel configurations continue to appear.

Gas uptake measurements are made by measuring pressure, temperature and, in some cases, composition of the fluid phases. On the other hand, information such as hydrate structure, composition, and cage occupancy are obtained from molecular level studies. It has been observed by Moudrakovski et al.[21] that quantitative measurement of kinetic processes in subvolumes (in this case, by following the disappearance of the liquid phase) of a larger sample suggests that the smaller the size of the volume observed becomes, the more inhomogeneous the process appears to be. Powder X-ray diffraction (PXRD) and Raman and Nuclear Magnetic Resonance (NMR) spectroscopy are the well-known tools used for solid phase structural analysis at a molecular level, also for gas hydrates.[22–27] Susilo et al.[27] have successfully used these techniques to characterize structure H hydrates of methane and several large organic molecules. Because of the different environments provided by each cage, both Raman and NMR spectra show that some gas/liquid signals are shifted when a molecule is encaged in a hydrate phase. Methane hydrate has been studied extensively. The signature of methane molecules in all three hydrate structures is shifted to a lower frequency in Raman[28] and to lower field in ^{13}C NMR[2,29] compared to the free gaseous state. It is accepted that analysis by Raman spectroscopy on gas hydrates is qualitative in nature. However, Raman spectroscopy sometimes can be used for quantitative determination of hydrate composition and cage occupancy if all peaks can be assigned unambiguously and intensities are calibrated for the specific system under study.[2,13,28] ^{13}C methane chemical shifts from NMR are more structure specific and the intensities are quantitative if the correct data acquisition experiment is used, and this makes the technique very useful in determining the cage occupancies in mixed gas hydrate systems. Both NMR and Raman gave comparable cage occupancy values for methane in structure I (sI) hydrate[30,31] yet a discrepancy was reported for a mixed hydrate with carbon dioxide, at least for one sample.[31] Gas hydrate crystal formation synthesized from the CH_4/C_2H_6, CH_4/C_3H_8, and $CH_4/C_2H_6/C_3H_8$ gas mixtures is studied in this work. This information is of interest for the development of technology for natural gas storage and transportation known as gas-to-solids technology.[32–34] To facilitate the development of

Table 1. Incipient Equilibrium Hydrate Formation Conditions

System	Temperature (K)	Incipient Equilibrium Pressure (MPa)	Gas Phase Composition (Mole Fraction) (Uncertainty ± 0.001)	
			Feed Gas	At Equilibrium
$CH_4/C_2H_6/H_2O$	273.7	1.43	CH_4 = 0.910 C_2H_6 = 0.090	CH_4 = 0.918 C_2H_6 = 0.082
$CH_4/C_3H_8/H_2O$	273.7	0.52	CH_4 = 0.905 C_3H_8 = 0.095	CH_4 = 0.904 C_3H_8 = 0.096
$CH_4/C_2H_6/C_3H_8/H_2O$	273.7	0.75	CH_4 = 0.902 C_2H_6 = 0.053 C_3H_8 =0.045	CH_4 = 0.904 C_2H_6 = 0.052 C_3H_8 = 0.044

these processes, data on the kinetics of hydrate growth coupled with compositional analysis of the gas phase are needed. The purpose of this study is to provide such information and discuss the implications for process design. Kinetics of hydrate formation for CH_4/C_2H_6, CH_4/C_3H_8, and $CH_4/C_2H_6/C_3H_8$ are studied by coupling gas uptake measurements with compositional analysis using gas chromatography. The kinetics of individual gases occupying different cages for the ternary system is also studied at a molecular level by *in-situ* Raman spectroscopy. This study also uses the three solid-state analytical tools (PXRD, NMR, and Raman) along with the information obtained by gas chromatography to identify the hydrate composition and cage occupancy of mixed gas hydrate of $CH_4/C_2H_6/C_3H_8$. As noted earlier, Uchida et al.[14] have recently reported the structure of the hydrates formed from the CH_4/C_3H_8 and $CH_4/C_2H_6/C_3H_8$ mixtures. However, they did not confirm the results by an independent method such as NMR and did not study the kinetics of hydrate growth.

Experimental Section

Gas uptake measurement

The gas mixtures used in this study were UHP grade and were supplied by Praxair Technology. The dry molar (%) gas compositions of the binary gas mixtures were determined by gas chromatography and are as follows: CH_4 (91.0)/C_2H_6 (9.0), CH_4 (90.5)/C_3H_8 (9.5). The dry molar (%) gas composition of the ternary gas mixture was: CH_4 (90.2)/C_2H_6 (5.3)/C_3H_8 (4.5). The water used was distilled and de-ionized.

The apparatus is the one used by Lee et al.[35] and Linga et al.[4] It consists of a crystallizer (CR) immersed in a temperature-controlled bath and equipped with the appropriate instrumentation to carry out hydrate formation at constant temperature and pressure using a fixed amount of water and a continuous supply of gas from a supply vessel (SV). The kinetics of hydrate formation was studied through gas uptake measurements following a technique pioneered in Bishnoi's laboratory.[36,37] The gas uptake method was coupled with gas phase composition measurements. All experiments were carried at pressures above the equilibrium pressure to ensure a finite rate of hydrate growth. The deviation of the experimental pressure or subcooling temperature from the equilibrium value is frequently called the *driving force*. The equilibrium pressures for the gas mixtures at 273.7 K were determined by following the isothermal pressure search method.[38] The results are shown in Table 1.

Hydrate phase characterization

The gas mixture used to form gas hydrate was UHP grade supplied by Praxair Technology. The dry molar gas composition was 88.5% CH_4, 6.9% C_2H_6, and 4.6% C_3H_8. Hydrates were synthesized from samples of 5 g of freshly ground ice particles that were poured by gravity into a 50 ml pressure vessel. The vessel has several spherical steel balls, which impart mixing and grinding to the sample when the vessel is kept on a rolling mill. The loading procedure was performed in a freezer at approximately 253 K to prevent melting of the ice. The zero time of the measurement was recorded when the vessel was pressurized to the desired pressure. Experiments were performed at 253 K or 270 K for 48 h. At the end of the 48-h period the temperature was increased to a point above the ice point (274 K) within 5 min in order to enhance the conversion of the remaining ice into hydrate.[27] The system was kept at 274 K for 24 h and then brought back to 253 K or 270 K until there is no change in pressure (almost full hydrate conversion was achieved). The starting pressure in each experiment was 2.8 MPa, and as the experiments were carried out in a batch mode the final pressure in the vessel was about 2.1 MPa. At the end of the experiment, the hydrate samples were collected under liquid nitrogen temperature (approximately 77 K). The recovered hydrate samples were kept in liquid nitrogen for subsequent analysis. For one experiment, hydrates were allowed to grow at 270 K for 48 h and then the temperature was increased to 283 K. The system was kept at 283 K for 24 h (until the pressure became constant) and the sample was collected at liquid nitrogen temperature for further analysis by Raman spectroscopy.

Crystal structure and lattice constant information were obtained from powder X-ray diffraction (PXRD). The PXRD measurements were performed with the $\theta/2\theta$ step scan mode and a counting time of 47.3 s/step and a step width of 0.041° in the 2θ range of 7–50° (40 kV, 40 mA; BRUKER axs model D8 Advance) using CuKα radiation (λ = 1.5406) (at163 K to prevent hydrate dissociation). The temperature deviation of the sample during measurement was within 1.0 K. The crystal information was then correlated to results from ^{13}C magic angle spinning (MAS) NMR at 173 K and Raman spectroscopy at liquid nitrogen temperature. A Bruker DSX 400 MHz NMR spectrometer was used to analyze the cage occupancies of the individual gases in the mixture, and hence, the hydrate structure. NMR measurements were performed on powdered hydrate samples; hydrate was packed in a 7 mm zirconia rotor, which was loaded into a variable

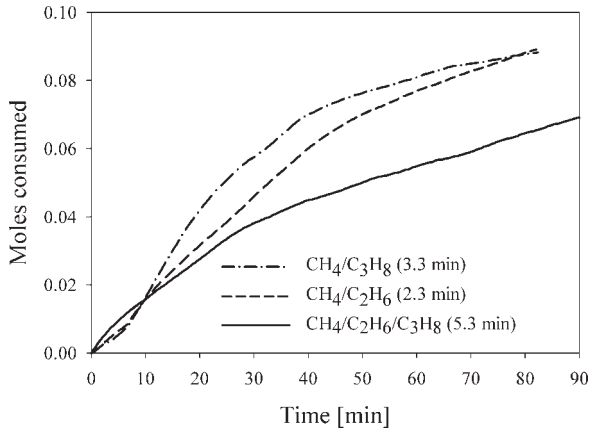

Figure 1. Gas uptake curves for CH_4/C_2H_6 (experiment 1, Table 2), CH_4/C_3H_8 (experiment 4, Table 2), and $CH_4/C_2H_6/C_3H_8$ (experiment 8, Table 2) with the corresponding induction times.

temperature probe. The spectra were recorded with magic angle spinning at 2.5 kHz spinning rate. A single pulse excitation (90° of 5 μs) and pulse repetition delay of 300 s under proton decoupling was employed. The cross polarization (CP MAS NMR) technique was also employed to distinguish the signals arising from the solid or liquid phase from those of the hydrate phase.

The synthetic hydrate samples were also analyzed using Raman spectroscopy. An Acton Raman spectrograph with fiber optics and equipped with a 1200 grooves/mm grating and a CCD detector was used in this study. An Ar-ion laser was used as the excitation source, emitting at 514.53 nm. The laser was focused on the sample by a 10× microscope objective. The spectrograph was controlled with a computer and the spectra were recorded with a 1 s integration time over 50 scans. All spectra were referenced to methane gas at 2918 cm^{-1}.

In situ Raman setup

The experimental pressure vessel (cell) used for in situ Raman measurement was made of 316 SS and has a volume of 1 cm^3. The vessel has a quartz window at the top and can operate at maximum pressure of 5 MPa. The temperature was kept constant by circulating cooling liquid through the channels made in the vessel for temperature control. In these experiments, the cell was loaded with approximately 0.2 g of crushed ice at 253 K. Subsequently, cooling liquid (50:50, w/w methanol-water) was circulated at 268 K (experimental temperature). The temperature inside the cell was measured by a thermocouple (±0.1 K). The cell was flushed three times with the gas mixture to remove any air present as impurity and then finally pressurized at the experimental pressure of 2.8 MPa. The cell window was then kept under the microscope of the Raman spectrometer to observe the change in Raman spectra with respect to time. A spectrum was recorded every 5 min by accumulating 50 scans (~1 min).

Results and Discussion

Table 1 shows the incipient gas hydrate formation conditions for the three mixtures at 273.7 K. Figure 1 shows gas uptake curves from three experiments corresponding to the CH_4/C_2H_6 and CH_4/C_3H_8 binary gas mixtures and the ternary mixture. The curves conform to the behavior of a gas uptake curve described by Bishnoi and Natarajan.[15] The rate of hydrate growth (R_f) is defined operationally as the slope of the gas uptake curve during the first 20 min after the induction time.[4,35] The two methane-containing binary systems exhibit similar growth rates initially possibly due to the fact that the methane content is the same and large compared to that of the other gas components. Subsequently, the propane-containing system exhibited fastest gas consumption but just prior to 80 min reaction time the ethane system had consumed the same amount of gas. The ternary system exhibited the least overall consumption as time passed. Considering that this is a more representative model of natural gas, this kinetic behavior is not favorable if one is interested in converting large amounts of natural gas into hydrate.

Hydrate formation from the CH_4/C_2H_6 mixture

As seen from Table 1, the minimum pressure to form hydrate crystals for this gas mixture at 273.7 K is 1.43 MPa. Gas uptake measurements for this system were taken at 273.7 K and at 2.9 and 3.9 MPa. Table 2 summarizes the results. As seen, nucleation occurred during the first 5 min and the induction times did not correlate with the driving force. Considering that the induction times are all within 3 min of each other, this is not surprising as the induction time has a random component.[16] Furthermore, the calculated

Table 2. Experimental Conditions Along with Measured Induction Times and Hydrate Formation Rates at 273.7 K

System	Exp. No.	Sample State	Driving Force* (MPa)	P_{exp} (MPa)	Induction Time (min)	Moles Consumed at Nucleation Point (Induction Time)	R_f† (mol/min)
($CH_4/C_2H_6/H_2O$)	1	Fresh	2.5	3.9	2.3	0.003	0.0017
	2	Fresh	1.5	2.9	4.7	0.006	0.0014
	3	Fresh	1.5	2.9	2.7	0.007	0.0016
($CH_4/C_3H_8/H_2O$)	4	Fresh	2.5	3.0	3.3	0.004	0.0025
	5	Fresh	1.5	2.0	3.3	0.002	0.0014
	6	Fresh	2.5	3.0	2.0	0.001	0.0011
	7	Fresh	1.5	2.0	3.3	0.003	0.0010
($CH_4/C_2H_6/C_3H_8/H_2O$)	8	Fresh	1.65	2.4	5.3	0.001	0.0012

*Driving force = $P_{exp} - P_{eq.}$
†Rate of hydrate growth (gas consumption rate for the first 20 min after nucleation).

Table 3. Vapor Phase Composition During Hydrate Formation from CH_4/C_2H_6 Mixture

$CH_4/C_2H_6/H_2O$ at 3.9 MPa (Experiment 1, Table 2)		$CH_4/C_2H_6/H_2O$ at 2.9 MPa (Experiment 2, Table 2)	
Sampling Time (min)	CH_4 Mole Fraction in Crystallizer (Uncertainty ± 0.001)	Sampling Time (min)	CH_4 Mole Fraction in Crystallizer (Uncertainty ± 0.001)
0.0	0.910	0.0	0.910
3.3	0.910	4.0	0.910
10.0	0.911	22.0	0.916
22.0	0.912	42.0	0.931
32.0	0.914	62.0	0.941
42.0	0.915	137.0	0.956
52.0	0.916	–	–
62.0	0.917	–	–
72.0	0.918	–	–
82.0	0.918	–	–

rates of growth are all of the same magnitude considering the uncertainty in the mole calculations.[4]

Gas phase analysis was conducted for experiments 1 and 2 and the results are shown in Table 3. Interestingly, the CH_4 gas content remains practically constant at 3.9 MPa but increases at 2.9 MPa. As CH_4 and/or C_2H_6 are consumed for hydrate formation the pressure drops and more gas is supplied from the Supply Vessel (SV) to maintain constant pressure (semi-batch operation). The fate of the two hydrate forming gases was calculated from kinetic information and gas chromatographic analysis and is shown in Figures 2 and 3. The description of the procedure to calculate the number of moles of the individual species is presented elsewhere.[4] As seen, the composition ratio (CH_4/C_2H_6) at 3.9 MPa increases during the first 25 min to about 9 and then begins dropping to about 7.8 in 80 min. On the other hand the composition ratio (CH_4/C_2H_6) drops more rapidly when hydrates form at 2.9 MPa (lower driving force). It is difficult to say whether any structural transitions occur over these times. Methane and ethane form structure I hydrate but a mixture of the two can form structure II.[2] Uchida et al.[13] have reported that, based on spectroscopic measurements for a binary mixture, of CH_4/C_2H_6 with a composition of C_2H_6 ranging between 2% and 22% both structure I and II coexist.

Hydrate formation from the CH_4/C_3H_8 mixture

As seen in Table 1 the minimum pressure to form hydrate crystals from this gas mixture at 273.7 K is 0.52 MPa. Gas uptake measurements for this system were obtained at 273.7 K and at 2.0 and 3.0 MPa. Table 2 summarizes the results. As seen, all the induction times are within a 4 min. range. It is noted that the induction time in experiment 6 was 2 min and the number of moles consumed at that point is 0.001 which is much lower than in experiment 4 (0.004). This reaffirms the fact that prediction of the kinetics of nucleation is difficult and that induction time prediction is not yet possible.

Gas phase analysis results are given in Table 4. It is evident from the table that the gas phase in the reactor is enriched with methane as the experiment proceeds. As seen from Figures 4 and 5, the composition ratio (CH_4/C_3H_8) drops more rapidly when hydrates form at 2 MPa (lower driving force). It is also interesting to note that while the amount of methane incorporated into hydrate is more at 3 MPa, the amount of propane is practically the same. Moreover, the amount of propane has reached a plateau within 60 min at 3 MPa and 100 min at 2 MPa. It appears that further growth is simply due to methane hydrate formation.

Hydrate formation from the $CH_4/C_2H_6/C_3H_8$ mixture

Gas uptake measurements were conducted at 273.7 K and 2.4 MPa. This pressure is 1.65 MPa above the incipient equilibrium pressure at 273.7 K (Table 1). The induction time was 5.3 min and the calculated rate during the first 20 min was found to be 0.0012 mol/min (Table 2). This rate is

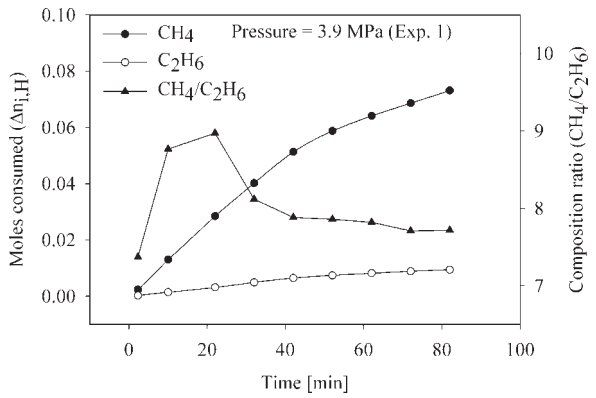

Figure 2. Mole consumption and molar ratio for the $CH_4/C_2H_6/H_2O$ system 3.9 MPa.

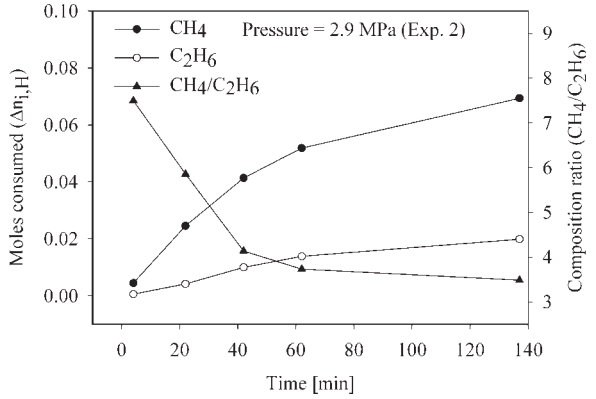

Figure 3. Mole consumption and molar ratio for the $CH_4/C_2H_6/H_2O$ system 2.9 MPa.

Table 4. Vapor Phase Composition During Hydrate Formation from CH_4/C_3H_8 Mixture

$CH_4/C_3H_8/H_2O$ at 3.0 MPa (Experiment 4, Table 2)		$CH_4/C_3H_8/H_2O$ at 2.0 MPa (Experiment 5, Table 2)		$CH_4/C_3H_8/H_2O$ at 2.0 MPa (Experiment 7, Table 2)	
Sampling Time (min)	CH_4 Mole Fraction in Crystallizer (Uncertainty ± 0.001)	Sampling Time (min)	CH_4 Mole Fraction in Crystallizer (Uncertainty ± 0.001)	Sampling Time (min)	CH_4 Mole Fraction in Crystallizer (Uncertainty ± 0.001)
0.0	0.905	0.0	0.905	0.0	0.905
3.7	0.908	3.0	0.906	5.0	0.911
12.0	0.912	12.0	0.910	10.0	0.912
22.0	0.919	22.0	0.943	20.0	0.916
32.0	0.931	32.0	0.948	30.0	0.927
42.0	0.939	42.0	0.957	40.0	0.934
52.0	0.941	52.0	0.968	50.0	0.940
62.0	0.942	62.0	0.978	70.0	0.956
72.0	0.944	72.0	0.984	100.0	0.983
82.0	0.945	82.0	0.987	120.0	0.991
–	–	92.0	0.991	–	–
–	–	132.0	0.994	–	–
–	–	640.0	0.997	–	–
–	–	660.0	0.997	–	–

within the range found for the constituent binary systems. Gas phase analysis results are given in Table 5 which shows that the concentration of CH_4 in the gas phase was much higher by the end of the experiment, close to 98% CH_4. Because of the increase in methane content of the gas phase, the rate of hydrate growth decreases as the equilibrium formation pressure increases, which in-turn decreases the driving force. Perhaps this is one of the reasons why the rate decreases continuously after nucleation. Considering that methane enrichment was also significant in the propane-containing binary system it appears that propane incorporation into the hydrate is a dominant factor. Figure 6 shows equal amounts of ethane and propane consumed. It is expected that experiments done at even lower pressures should be able to give a gas phase almost free of propane and ethane. However, the rate of growth does become much smaller.

Hydrate phase characterization

Synthetic hydrate samples were analyzed by PXRD first to confirm the presence of hydrate and to verify the crystal structure. A PXRD pattern of the sII hydrate product made with CH_4 (88.5 mol %)/C_2H_6 (6.9 mol %)/C_3H_8 (4.6 mol %), as obtained in our experiment is shown in Figure 7. The presence of ice is indicated by the asterisk. It was found that the gas mixture always formed structure II hydrate under the temperature and pressure conditions studied. The pattern was fitted to a standard sII hydrate pattern (space group Fd3m) to obtain the lattice constants and unit cell volumes. The synthetic mixed hydrate sample analyzed at 163 K and atmospheric pressure has a unit cell constant of 17.23 Å and cell volume of 5115 Å.^{3} Diffraction of the sample also was observed with increasing temperature, the increment being 5 K, in order to see at which temperature all of the hydrate disappeared. The rate of increase in temperature was approximately 2.5 K per minute. It was observed that (results not shown) at this rate all of the hydrate dissociated at around 213 K (±2 K). Once the PXRD measurements confirmed that the solid phase contained hydrate, the hydrate phase composition was obtained by gas chromatography. Table 6 shows the gas/hydrate composition at each stage. As shown in Table 6 by the end of the experiment gas phase is almost 99% methane. This is in agreement with the gas phase composition from the gas uptake measurements shown in Table 5.

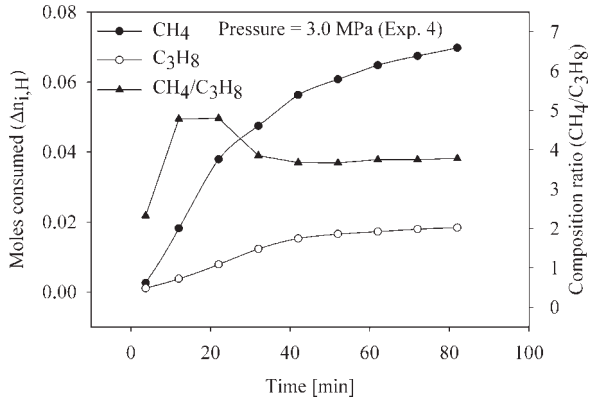

Figure 4. Mole consumption and molar ratio for the $CH_4/C_3H_8/H_2O$ system at 3.0 MPa.

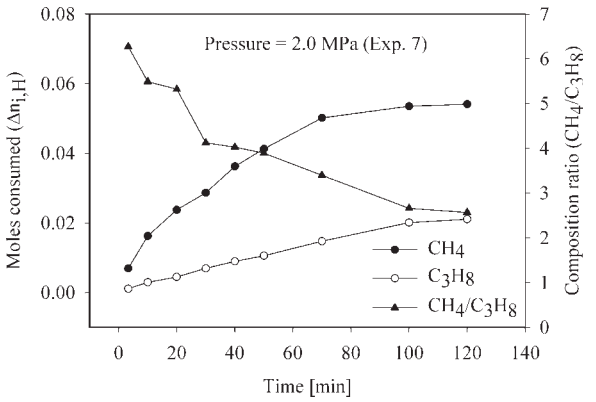

Figure 5. Mole consumption and molar ratio for the $CH_4/C_3H_8/H_2O$ system at 2.0 MPa.

Table 5. Vapor Phase Composition During Hydrate Formation from $CH_4/C_2H_6/C_3H_8$ Mixture

$CH_4/C_2H_6/C_3H_8/H_2O$ at 2.4 MPa (Experiment 8, Table 2) (Uncertainty ± 0.001)			
Sampling Time (min)	CH_4 Mole Fraction in Crystallizer	C_2H_6 Mole Fraction in Crystallizer	C_3H_8 Mole Fraction in Crystallizer
0.0	0.903	0.053	0.044
10.0	0.904	0.052	0.044
20.0	0.918	0.047	0.035
30.0	0.930	0.043	0.027
40.0	0.937	0.039	0.024
50.0	0.945	0.035	0.020
60.0	0.949	0.033	0.018
80.0	0.959	0.030	0.011
100.0	0.961	0.027	0.012
120.0	0.966	0.025	0.009
180.0	0.974	0.019	0.007
200.0	0.978	0.018	0.004

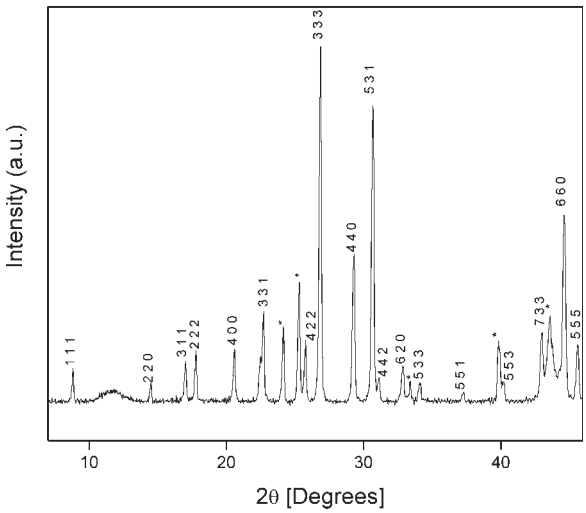

Figure 7. PXRD pattern of sII hydrate performed at 163 K on hydrate sample synthesized by $CH_4/C_2H_6/C_3H_8$ mixture at 2.8 MPa and 270 K.

Hydrates synthesized in the rolling cell reactor at 253 and 270 K at an initial pressure of 2.8 MPa were studied with Raman spectroscopy at liquid nitrogen temperature and atmospheric pressure, thus marking the signals of individual gas components in hydrate cages. Guest molecules trapped in hydrate cages may have hydrate structure-specific and cavity-specific signatures in terms of the Raman bands being shifted from gas phase values. Raman spectra for methane and other natural gases in different hydrate structures and phases have been studied[13,14,18,28] extensively. Figure 8 shows a typical Raman spectrum of the C—H (2800–3000 cm^{-1}) and O—H regions (3000–3400 cm^{-1}) of the gas hydrate. The spectrum supports the conclusions obtained from XRD analysis that the hydrate is structure II. Two large peaks at approximately 2904 cm^{-1} and 2914 cm^{-1} indicate CH_4 molecules encaged in large cages and small cages, respectively. Other small peaks in the region 2850–3000 cm^{-1} are from ethane and propane in the large cages. These peaks have a relatively low signal-to-noise ratio due to the presence of the small amounts of these gases in the resultant hydrate structure. Two large, broad peaks at approximately 3090 cm^{-1} and 3220 cm^{-1} are due to the internal vibrational modes of water molecules making up the host lattice of the hydrate structure.[24] Additionally, a minor band for methane was present at about 3050 cm^{-1} indicative of methane in the hydrate phase.[7] This peak is due to the Raman active CH_4 mode (v_3), which occurs at 3026 cm^{-1} in pure methane at 90 K.[24]

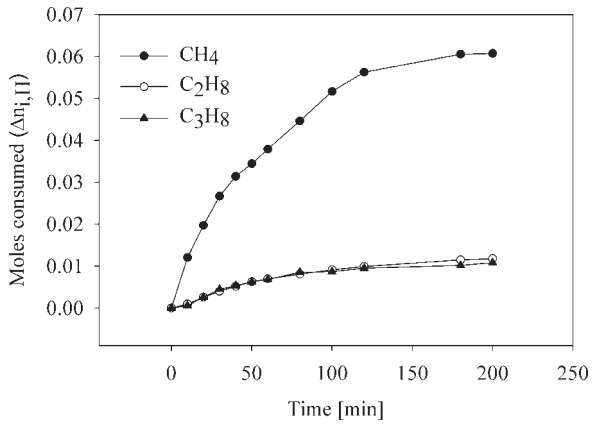

Figure 6. Mole consumption for the $CH_4/C_2H_6/C_3H_8/H_2O$ system at 2.4 MPa.

Figure 9 shows the C—H spectral region obtained for three different experiments at 253 K, 270 K, and 283 K and the same initial pressure of 2.8 MPa. The Raman band at 2903 cm^{-1} was assigned to the C—H stretching mode of methane in the large cage of structure II. The peak at 2914 cm^{-1} is for methane in the small cage. It has been observed that propane and ethane only occupy the large cages of structure II. The C—H stretching vibrations of propane in the large cages appears at around 2870, 2878, 2984, 2900, and 2920 cm^{-1} as observed from the measurement on pure propane hydrate. However, for a methane/ethane/propane system, only the first three propane peaks mentioned earlier are visible as they have stronger signals compared to the last two and they do not overlap with the strong methane signals at 2903 and 2914 cm^{-1} as shown in Figure 9. Moreover, at higher temperature (Figure 9c), propane dominates the hydrate phase composition over methane and hence the propane signal at 2920 cm^{-1} becomes more evident as seen on the right shoulder of the methane peak at 2914 cm^{-1}. Hydrate peaks for ethane were observed at 2885 and

Table 6. Phase Composition at Start and End of the Experiment as Analyzed by Gas Chromatography

Description	Methane (mol %)	Ethane (mol %)	Propane (mol %)
Feed gas composition (start)	88.5 (±0.2)	6.9 (±0.2)	4.6 (±0.2)
Gas phase composition (end)	98.8 (±0.2)	0.9 (±0.2)	0.3 (±0.2)
Hydrate phase composition	69.1 (±0.2)	18.2 (±0.2)	12.7 (±0.2)

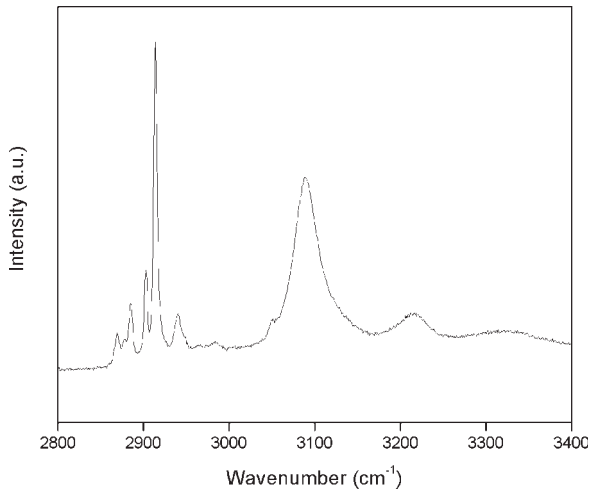

Figure 8. Typical Raman spectra for the mixed hydrate of methane, showing the C—H stretching region for hydrate guest molecule between 2800 and 3000 cm^{-1}.

Also note the broad water band for O—H stretching between 3000 to 3400 cm^{-1}. Spectra were obtained at liquid nitrogen temperature. Hydrate was synthesized at 253 K.

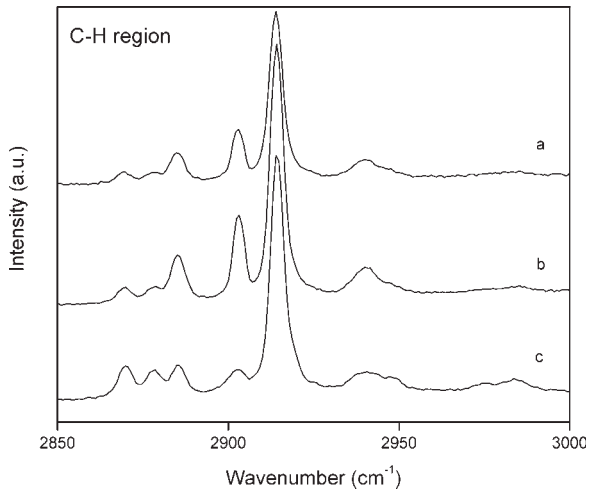

Figure 9. Raman spectra of hydrate measured at liquid nitrogen temperature showing C—H stretching regions for the hydrate guests.

(a) Hydrate synthesized at 253 K and 2.8 MPa, (b) hydrate synthesized at 270 K and 2.8 MPa, and (c) hydrate synthesized at 283 K and 2.8 MPa.

2940.5 cm^{-1}. There is no major difference between the spectra obtained at 253 and 270K. The intensity ratio of methane in the large cage to that of the small cage is similar. On the basis of this information it can be said that cage occupancy of hydrates synthesized at 253 K is similar to the cage occupancy of hydrates synthesized at 270 K. However, the spectrum at 283 K is different. The intensity ratio of methane in large to small cages is smaller compared to the experiments performed at 270 K and 253 K. Also, the peak intensity for propane occupying the large cages is significantly higher. This suggests that the cage occupancy of the mixed hydrate synthesized at 283 K is different from the hydrates synthesized at 253 K and 270 K. The above results indicate that at higher temperatures propane occupies the large cages preferentially and most of the methane occupies only the small cages. Similar results were obtained while comparing the C—C stretching mode as shown in Figure 10.

Figure 10 shows the C—C stretch mode region for propane and ethane in the hydrate cages. The Raman stretching mode at 992.5 cm^{-1} is assigned to ethane in large cages, and the Raman-active stretching mode of propane is observed at three different positions. The main peak is at 878.5 cm^{-1} with two small ones at 1054 and 1157.5 cm^{-1}. These numbers match well with literature values.[7,25] Table 7 shows the peak positions of each gas reported in this work. Although the C—C bands are weaker compared to those in the C—H stretch region, they can still be used to comment on the intensity ratio of propane to ethane peaks. It has been observed that the peak intensity ratio for ethane to propane is almost similar for experiments done at 253 K and 270 K. However, for the experiment carried out at 283 K the peak intensity ratio of ethane to propane is lower. It has also been observed from the gas uptake measurements that the mole fraction of CH_4 in the vapor phase increases as hydrate crystallization progresses, especially when the driving force is smaller.

In situ Raman analysis

Results of a typical time-resolved *in-situ* Raman experiment are shown in Figure 11a. The peak observed at 2918 cm^{-1} at zero time arises purely from methane gas present amongst the porous ice powder. The Raman peak for methane gas trapped in the small cages of structure II starts appearing at 2914 cm^{-1} as a shoulder on the gas peak and keeps growing until it can be seen as a resolved shoulder within 1 h of the start of hydrate formation. Methane also occupies the large cages of structure II, and a small peak can be seen at 2903 cm^{-1} as a shoulder on the peak for methane in small cages. A distinct

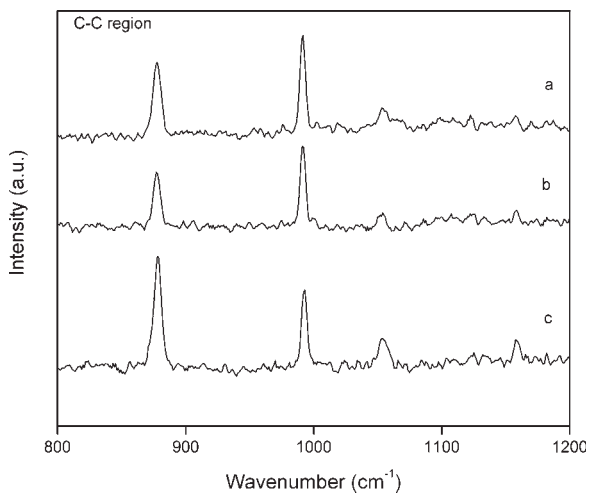

Figure 10. Raman spectra of hydrate measured at liquid nitrogen temperature showing C—C stretching regions of the hydrate guests.

(a) Hydrate synthesized at 253 K and 2.8 MPa, (b) hydrate synthesized at 270 K and 2.8 MPa, and (c) Hydrate synthesized at 283 K and 2.8 MPa.

Table 7. Reported Raman Wavenumbers for Synthesized $CH_4/C_2H_6/C_3H_8$ sII Hydrate

Description	Component	Wavenumber (cm^{-1})
C—H stretching region	Methane (hydrate)	~2903 (Large cages in sII)
	Methane (hydrate)	~2914 (Small cages in sII)
	Ethane (hydrate)	~2885, 2940.5 (All large cages in sII)
	Propane (hydrate)	~2870, 2878.5, 2984 (All large cages in sII)
	Methane (gas)	~2918
C—C stretching region	Ethane (hydrate)	~992.5 (Large cages in sII)
	Propane (hydrate)	~878.5, 1054, 1157.5 (All large cages in sII)
	Ethane (gas)	~994.5
	Propane (gas)	~871.3

shoulder for methane in the large cages of structure II can be seen at a later time during hydrate formation. Figure 11b shows the intensity ratio of signals for methane in small cages to that of free methane in the surrounding gas. The intensity ratio reported here has been averaged over three different runs for similar systems. The result suggests that the total amount of methane in small cages increases linearly with time. Figure 11c shows how the intensity ratio of signals for methane in the large cages to that of methane in small cages changes with time. As seen at the start of the experiment, the rate of growth of the methane population in the large cages of structure II is faster than the rate at which methane populates the small cages. It has also been seen that the contribution from ethane and propane seems to become more dominant when hydrate is allowed to equilibrate for 24 h. This might suggest that hydrate is originally formed with a large amount of methane in the $5^{12}6^4$ cavities, which is exchanged over time for ethane and propane. This explains the observation in Figure 11c that initially the rate of methane gas going into large cages is faster compared to methane going into the small cages. It is also noted for the gas uptake measurements, as seen in Figures 2–5, that the initial rate of methane incorporation into the hydrate phase is faster. Hence hydrate samples taken at different times during a kinetic experiment will enable us to "tune" the compositions of the resultant hydrate to a certain extent.

Figure 12 shows the time-resolved C—C stretching mode of ethane and propane in the hydrate phase. As seen, the propane peak at 878.5 cm^{-1} and the ethane peak at 992.5 cm^{-1} in the hydrate phase grow with time. Figure 12 also shows the peak position of ethane and propane in the gas phase. As

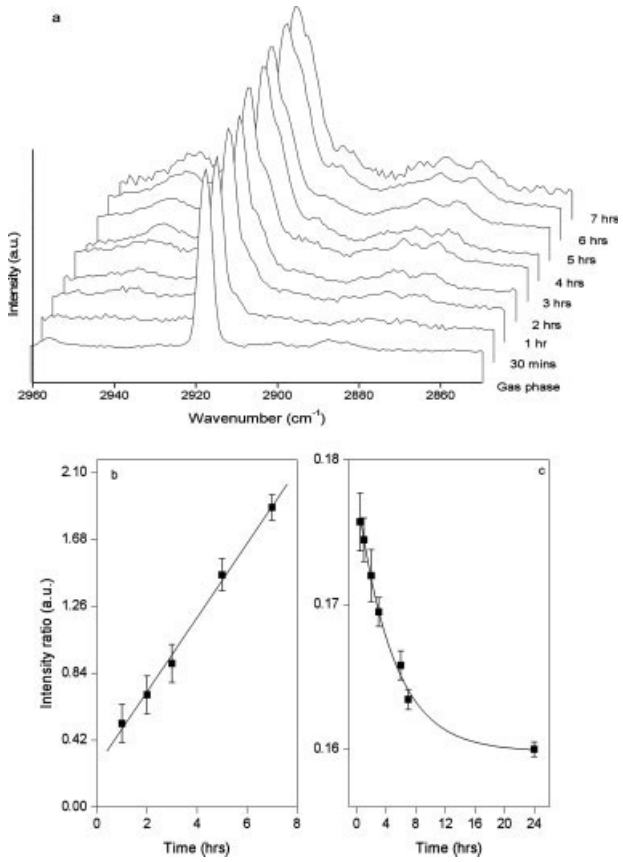

Figure 11. *In situ* Raman spectra of the C—H region for $CH_4/C_2H_6/C_3H_8$ hydrates obtained at 268 K and 2.8 MPa.

(a) Note the peak for methane in small cages (as a shoulder on the main peak of methane in the gas phase increasing with time). (b) Intensity ratio of the peak for methane in small cages to that of methane in the gas phase. (c) Intensity ratio of methane in large cages to that of the small cages.

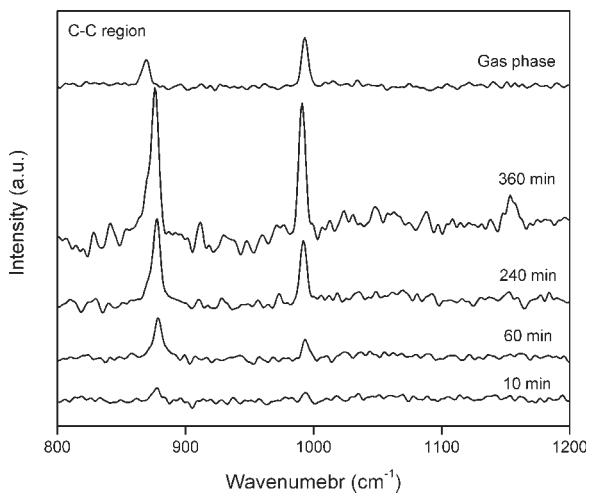

Figure 12. *In situ* Raman spectra of the C—C region for $CH_4/C_2H_6/C_3H_8$ hydrates obtained at 268 K and 2.8 MPa.

Note the propane peak positions in hydrate phase is at higher wavenumber compared to the gas phase.

seen, the C—C stretching mode of propane in the hydrate phase shifts to higher wavenumber as compared to the that in the gas phase, whereas the ethane signal from the hydrate phase shifts to lower wavenumber compared to that of the free gas phase. This result is consistent with the values reported in the literature.[2,28]As seen in Figure 12, a lower concentration of propane in the gas phase results in a smaller peak as compared to that for ethane. In the hydrate phase, the peak for propane is bigger as compared to that for ethane. Comparing the peak intensities of ethane and propane in the large cages of structure II, it can be said that propane is the preferred guest for the large cages.

Uchida et al.[14] reported that the preferential enclathration in the $5^{12}6^4$ cage is $CH_4 < C_2H_6 < C_3H_8$. Our work confirms this and based on the *in situ* Raman studies suggests that kinetics controls the rate of methane occupancy of the large cages of structure II as compared to the small cages (Figure 11c).

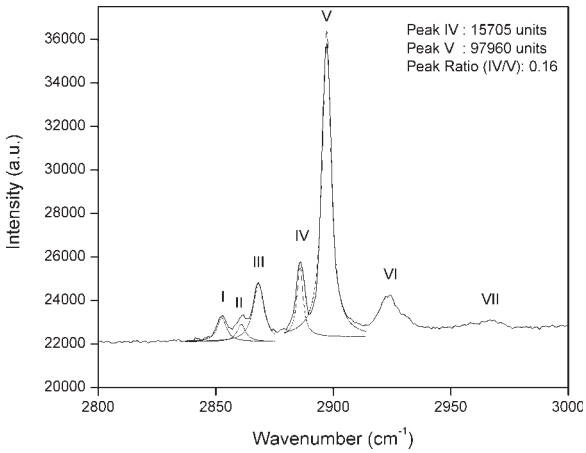

Figure 13. Absolute peak intensity of methane peaks from typical Raman spectra conducted at liquid nitrogen temperature on hydrate sample synthesized at 270 K and 2.8 MPa.

Quantitative determination of the cage occupancy by Raman spectroscopy

It is generally accepted that Raman spectroscopy cannot be used to determine the relative concentration of different guests in the hydrates quantitatively. The intensity of the signal generated by a specific ethane vibrational mode is likely to differ in intensity from that of an equal number of the same vibrational modes in propane molecules. As well, because of possible differences in polarizabilities of molecules in different cages, including the effect of different guests in neighboring cavities, intensities for molecules in different cages are not directly comparable. However, we will assume that errors arising in systems with only weakly polar hydrocarbon guests are going to be small, and we can estimate the relative amounts of a guest molecule in the different cages of a hydrate by comparing integral peak intensities. Therefore, it is possible to estimate the cage occupancies of mixed hydrates with some additional information and a few wise assumptions.[28]

In this study we have used the information obtained by PXRD and gas chromatography, in addition to peak ratios of methane in small to large cages, as obtained by Raman spectroscopy to quantify the cage occupancy values of different gases in hydrate cages. The PXRD pattern obtained for the synthetic hydrate reveals that the hydrate is a pure structure II phase. Once the structure of the hydrate is determined, the hydrate sample is decomposed and analyzed by gas chromatography for overall hydrate composition. As shown in Table 6, in every 100 moles of gas leaving the decomposing hydrate, there are 69.10 moles of methane, 18.20 moles of ethane, and the rest is propane. By peak deconvolution, it is easier to calculate the peak ratio of methane in the large cages to that in the small cages of the resultant structure II hydrate. Figure 13 shows a typical Raman spectrum obtained from a hydrate sample at liquid nitrogen temperature. From the fitted curves of Figure 13, the ratio of the integrated intensities of methane in large cages (curve IV) to methane in the small cages (curve V) is 0.16. Assuming that the intensities can be compared directly and knowing that there are two times as many small as large cages in the structure II unit cell, the following two equations can be satisfied for the total amount of methane in the hydrate cages (obtained by gas chromatography) and the ratio of methane in large to small cages (obtained by Raman spectroscopy)

$$2\theta_{S-M} + \theta_{L-M} = 69.10 \quad (1)$$

$$\theta_{L-M}/2\theta_{S-M} = 0.16 \quad (2)$$

where $\theta_{S\text{-}M}$ *and* $\theta_{L\text{-}M}$ are methane occupancies in small and large cages of resultant sII hydrate. In writing the above equations, it has been kept in mind that ethane and propane should not occupy the small cages of structure II. Indeed, the positions of the Raman stretching modes of the C—H and C—C bonds study suggest that neither ethane nor propane actually are present in the small cages of structure II. Solution of Eqs. 1 and 2 gives 59.57 moles of methane in the small cages (equivalent to 89.3% occupancy) and 9.53 moles in the large cages. It is safe to assume that the large cages have to be completely filled to maintain hydrate stability. There are 9.53 moles of methane, 18.20 moles of ethane and 12.70 moles of propane in the large cages which give cage occupancies of 23.6% (methane), 45.0% (ethane) and 31.4% (propane) in the large cages. Table 8 reports these cage occupancies.

Uchida et al.[14] studied the $CH_4/C_2H_6/C_3H_8$ ternary mixture using Raman spectroscopy and gas chromatography. Their Raman spectroscopy results suggest that CH_4 molecules were not included in the $5^{12}6^4$ cages in the resultant mixed hydrate from mixtures with 90/5/5 and 92/4/4 mol % composition, although methane was detected in the large cages in the 98/1/1 mol % mixture. In this work, we used an 88.5% CH_4/6.9% C_2H_6/4.6% C_3H8 mixture. Our results show that methane does occupy the $5^{12}6^4$ hydrate cages along with ethane and propane. This is confirmed by gas chromatography, Raman, and NMR spectroscopies. There might be several factors which are responsible for these differences, like hydrate formation pressure and hydrate formation time. The relative magnitude of the ice and hydrate peaks at the XRD plot of the hydrate sample of Uchida et al.[14] show that the

Table 8. Cage Occupancy Values Obtained by Combination of Results from Raman & Gas Chromatography, Which Compares Well with Results Obtained with ^{13}C MAS NMR

Description	Hydrate Structure	Methane θ_S	Methane θ_L	Ethane θ_L	Propane θ_L	Hydration Number n
Raman + gas chromatography (mole balance calculation)	sII	0.893	0.236	0.450	0.314	6.10
C^{13} NMR, high power decoupling (statistical thermodynamic model)	sII	0.888	0.287	0.446	0.264	6.13

hydrate content of their sample is small. It is very important to understand these differences. The above findings further suggest that that one cannot use an equilibrium model to predict the product composition during a gas hydrate formation reaction, as there are kinetic and transport factors that will affect composition. It should be noted that it is not necessarily trivial to obtain a true equilibrium hydrate as this may require a number of formation-decomposition-reformation cycles under near-equilibrium conditions (T, P, composition).

NMR results for quantitative determination of cage occupancy

Figure 14 shows the ^{13}C magic angle spinning (MAS) NMR spectrum obtained at 173 K and 0.1 MPa with ~2.5 kHz spinning rate. High power proton decoupling was used to give quantitative spectra, but cross-polarization (CP) was also employed in this study. Chemical shift values for methane in both small and large cages of structure II match well with the literature.[2] It can be seen that the intensity of the peak from methane in small cages (−4.36 ppm) is much larger compared to that from methane in the large cages (at −8.25 ppm). This indicates that only a small fraction of large cages is filled with methane. In the same spectrum, propane, which occupies only the large cages of structure II, exhibits two distinct peaks. One peak corresponds to methyl carbons (at 17.5 ppm) and the other to the methylene carbon (at 16.75 ppm). Also, a peak from ethane in the large cages of structure II hydrate appears at 6.15 ppm. Table 9 summarizes the ^{13}C NMR shifts.

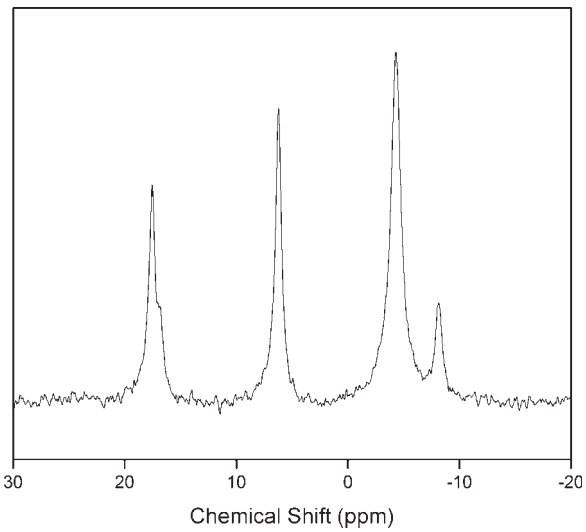

Figure 14. ^{13}C MAS NMR spectrum of sII hydrate conducted at 173 K on the hydrate sample, synthesized with $CH_4/C_2H_6/C_3H_8$ mixture at 2.8 MPa and 270 K.

CP MAS NMR spectra collected for the above system were identical to the one shown in Figure 14. However, ordinarily only high power proton decoupled spectra can give quantitative values of different gases in the individual hydrate cages and this only when the delay times in the experiment are set to appropriately long values. Because methane partitions between the small and large cavities of structure II, deconvolution of the band shown in Figure 14 was necessary. This procedure allowed the determination of the ratio of areas of the small to the large bands, and after accounting for the fact that, there are two times as many small as large cages in structure II, the occupancy ratio of methane in small to large cages (Eq. 3) was determined. Similarly, the ratio of peak intensities of ethane in large cages to methane in large cages (Eq. 4) and propane in large cages to methane in large cages (Eq. 5) can be calculated from the absolute peak intensity values.

The following ratios of peak intensities were obtained from the spectra information

$$\frac{\theta_{s(CH_4)}}{\theta_{l(CH_4)}} = r1 \tag{3}$$

$$\frac{\theta_{l(C_2H_6)}}{\theta_{l(CH_4)}} = r2 \tag{4}$$

$$\frac{\theta_{l(C_3H_8)}}{\theta_{l(CH_4)}} = r3 \tag{5}$$

To determine the absolute occupancy of individual gas in each cage, the statistical thermodynamics expression for the chemical potential $-\Delta\mu_w^o$ of water molecules in a structure II hydrate was invoked.

$$-\Delta\mu_w^o = \frac{RT}{n_{H_2O}} \sum_i \upsilon_i \ln(1-\theta_i)$$

$$-\Delta\mu_w^o = \frac{RT}{n_{H_2O}} \left[2\ln(1-\theta_{s(CH_4)}) + 1\ln(1-\theta_{l(CH_4)}-\theta_{l(C_2H_6)}-\theta_{l(C_3H_8)})\right] \tag{6}$$

where θ_S and θ_L are the fractional occupancy of small and large cages, respectively. Equation 6 assumes[28] (i) that the free energy of the hydrate is independent of the nature of the guest, (ii) each cavity can be occupied by only one guest

Table 9. Reported Chemical Shift for Synthesized $CH_4/C_2H_6/C_3H_8$ sII Hydrate by C^{13} NMR

Description	Component	Chemical Shift (ppm)
Chemical shift by high power decoupling	Methane (hydrate)	−4.36 (Small cages in sII)
	Methane (hydrate)	−8.25 (Large cages in sII)
	Ethane (hydrate)	6.15 (Large cages in sII)
	Propane (hydrate)	16.75, 17.5 (Both large cages in sII)

molecule, and the guest molecules cannot diffuse from the cavity, (iii) there are no guest–guest interactions or host-lattice distortions, (iv) classical statistics are valid, and (v) quantum effects do not need to be considered. The value for $\Delta\mu_w^o$ used in the calculation is 883.8.[18]

Therefore, by combining Eqs. 3–6, the occupancy of the small and large cages by individual gases was determined. The results are shown in Table 8, as well as the corresponding values calculated by Raman spectroscopy. The column labeled n in Table 8 corresponds to the hydration number calculated by the following expression:

$$n = \frac{n_{H_2O}}{2\theta_{s(CH_4)} + \theta_{l(CH_4)} + \theta_{l(C_2H_6)} + \theta_{l(C_3H_8)}} \quad (7)$$

The value of the hydration number obtained by NMR agrees well with the one obtained by Raman and with results from the literature.[18] The results obtained from ^{13}C NMR indicate that almost 100% of the large cages are filled, which confirms that the assumption we made for the cage occupancy calculation using Raman spectroscopy is valid. The cage occupancy values obtained from the Raman results are in good agreement with the quantitative results, which we obtained by ^{13}C NMR using high power proton decoupling.

Recommendation for process design

In an industrial process, rapid conversion of all natural gas into hydrate is desired. Thus, the observed fractionating effect will necessitate recycling of unconverted gas and, consequently, increase the compression costs and possible complications in the controllability of the process. A possible remedy is a two-step process that takes advantage of the fractionation effect in the first stage to recover almost pure methane which is then fed to the second stage. Thus, a facility to convert natural gas into hydrate for storage or transport would consist of two consecutive hydrate formations stages. Obviously, the second one with almost pure methane as feed would operate at a higher pressure.

Conclusions

Gas hydrates made from CH_4/C_2H_6, CH_4/C_3H_8, and $CH_4/C_2H_6/C_3H_8$ gas mixtures were formed at 273.7 K in a crystallizer operating with a fixed amount of water and a continuous supply of gas to maintain constant pressure. The methane concentration in the gas phase was found to increase during the experiments, especially in the propane-containing mixtures. This, unfortunately, raises the equilibrium formation pressure and thus reduces the driving force, which in turn reduces the rate of hydrate growth.

^{13}C NMR was used to determine the cage occupancies and hydration numbers for mixed hydrate from a methane/ethane/propane gas mixture. It was found that the large cages are almost fully occupied by a combination of all three gases and the small cages were about 90% occupied by methane. It was also shown that Raman spectroscopy could give similar information to that obtained from NMR spectroscopy, at least in this particular case, although one must always consider that Raman results need to be calibrated against a quantitative method such as NMR spectroscopy. However, Raman spectroscopy is simpler and less resource intensive compared to the NMR technique, making it more useful for monitoring gas hydrate formation in an industrial process. Some further conclusions are that the hydrate and gas composition vary as the reaction proceeds, giving a small measure of tunability of the composition. As well, this varying composition is unpredictable by equilibrium modeling software as kinetic and transport factors do affect the progress of the reaction in detail. The fractionation effect can be taken into account in the design of industrial natural gas hydrate storage and transport processes by employing two hydrate formation stages.

Acknowledgments

The financial support from the Natural Sciences and Engineering Research Council of Canada (NSERC) is greatly appreciated. We also thank Dr. Judong Lee for assistance with the collection of gas uptake data for the CH_4/C_2H_6 and CH_4/C_3H_8 mixed hydrates.

Literature Cited

1. Von Stackelberg M, Jahns W. Feste Gashydrate VIDie Gitterauweitungsarbeit. *Zeitschrift fur Elektrochemie*. 1954;58:162–164.
2. Subramanian S, Kini RA, Dec SF, Sloan ED. Evidence of structure II hydrate formation from methane plus ethane mixtures. *Chem Eng Sci*. 2000;55:1981–1999.
3. Uchida T, Moriwaki M, Takeya S, Ikeda IY, Ohmura R, Nagao J, Minagawa H, Ebinuma T, Narita H, Gohara K, Mae S. Two-Step formation of methane-propane mixed gas hydrates in a batch-type reactor. *AIChE J*. 2004;50:518–523.
4. Linga P, Kumar R, Englezos P. Gas hydrate formation from hydrogen/carbon dioxide and nitrogen/carbon dioxide gas mixtures. *Chem Eng Sci*. 2007;62:4268–4276.
5. Kawamura T, Sakamoto Y, Ohtake M, Yamamoto Y, Komai T, Haneda H, Yoon JH. Dissociation behavior of pellet-shaped methane hydrate in ethylene glycol and silicone oil. Part 1: dissociation above ice point. *Industrial Eng Chem Res*. 2006;45:360–364.
6. Kini RA, Dec SF, Sloan ED. Methane plus propane structure II hydrate formation kinetics. *J Phys Chem A*. 2004;108:9550–9556.
7. Schicks JM, Naumann R, Erzinger J, Hester KC, Koh CA, Sloan ED. Phase transitions in mixed gas hydrates: experimental observations versus calculated data. *J Phys Chem B*. 2006;110:11468–11474.
8. Uchida T, Ikeda IY, Takeya S, Kamata Y, Ohmura R, Nagao J, Olga ZY, Buffet BA. Kinetics and stability of CH_4-CO_2 mixed gas hydrates during formation and long-term storage. *Chem Phys Chem*. 2005;6:646–654.
9. Park Y, Lee J, Shin K, Seol J, Lee KM, Huh DG, Park KP, Lee H. Phase and kinetic behavior of the mixed methane and carbon dioxide hydrates. *Korean J Chem Eng*. 2006;23:283–287.
10. Svandal A, Kuznetsova T, Kvamme B. Thermodynamic properties and phase transitions in the $H_2O/CO_2/CH_4$ system. *Fluid Phase Equilib*. 2006;246:177–184.

11. Svandal A, Kuznetsova T, Kvamme B. Thermodynamic properties and phase transtions in the $H_2O/CO_2/CH_4$ system. *Phys Chem Chem Phys*. 2006;8:1707–1713.
12. Kida M, Sakagami H, Takahashi N, Hachikubo A, Shoji H, Kamata Y, Ebinuma T, Narita H, Takeya S. Estimation of gas composition and cage occupancies in CH_4-C_2H_6 hydrates by CP-MAS C-13 NMR technique. *J Jpn Pet Inst*. 2007;50:132–138.
13. Uchida T, Takeya S, Kamata Y, Ikeda IY, Nagao J, Ebinuma T, Narita H, Zatsepina O, Buffett BA. Spectroscopic observations and thermodynamic calculations on clathrate hydrates of mixed gas containing methane and ethane: Determination of structure, composition and cage occupancy. *J Phys Chem B*. 2002;106:12426–12431.
14. Uchida T, Takeya S, Kamata Y, Ohmura R, Narita H. Spectroscopic measurements on binary, ternary, and quaternary mixed-gas molecules in clathrate structures. *Ind Eng Chem Res*. 2007;46:5080–5087.
15. Bishnoi PR, Natarajan V. Formation and Decomposition of Gas Hydrates. *Fluid Phase Equilib*. 1996;117:168–177.
16. Englezos P. Nucleation and growth of gas hydrate crystals in relation to "kinetic inhibition". *Revue de l'Institut Francais du Petrole*. 1996;51:789–795.
17. Englezos P. Clathrate Hydrates. *Ind Eng Chem Res*. 1993;32:1251–1274.
18. Sloan ED Jr. *Clathrate Hydrates of Natural Gases*, 2nd ed. Revised and Expanded. NY: Marcel Dekker; 1998.
19. Koh CA. Towards a fundamental understanding of natural gas hydrates. *Chem Soc Rev*. 2002;31:157–167.
20. Clarke MA, Bishnoi PR. Determination of the intrinsic kinetics of CO_2 gas hydrate formation using in situ particle size analysis. *Chem Eng Sci*. 2005;60:695–709.
21. Moudrakovski IL, McLaurin GE, Ratcliffe CI, Ripmeester JA. Methane and carbon dioxide hydrate formation in water droplets: Spatially resolved measurements from magnetic resonance microimaging. *J Phys Chem B*. 2004;108:17591–17595.
22. Ripmeester JA, Ratcliffe CI. Low-temperature cross-polarization magic angle spinning C-13 NMR of solid methane hydrates—Structure, cage occupancy, and hydration number. *J Phys Chem*. 1988;92:337–339.
23. Ripmeester JA, Ratcliffe CI. On the contributions of NMR spectroscopy to clathrate science. *J Struct Chem*. 1999;40:654–662.
24. Tulk CA, Ripmeester JA, Klug DD. The application of Raman spectroscopy to the study of gas hydrates. *Ann N Y Acad Sci*. 2000;912:859–872.
25. Sloan ED. Clathrate hydrate measurements: microscopic, mesoscopic, and macroscopic. *J Chem Thermodyn*. 2003;35:41–53.
26. Susilo R, Moudrakovski IL, Ripmeester JA, Englezos P. Hydrate kinetics study in the presence of nonaqueous liquid by nuclear magnetic resonance spectroscopy and imaging. *J Phys Chem B*. 2006;110:25803–25809.
27. Susilo R, Ripmeester JA, Englezos P. Characterization of Gas Hydrates with PXRD, DSC, NMR and Raman Spectroscopy. *Chem Eng Sci*. 2007;62:3930–3939.
28. Sum AK, Burruss RC, Sloan ED. Measurement of clathrate hydrates via Raman spectroscopy. *J Phys Chem B*. 1997;101:7371–7377.
29. Seo YT, Lee H. C-13 NMR analysis and gas uptake measurements of pure and mixed gas hydrates: Development of natural gas transport and storage method using gas hydrate. *Korean J Chem Eng*. 2003;20:1085–1091.
30. Uchida T, Ohmura R, Ikeda IY, Nagao J, Takeya S, Hori A. Phase equilibrium measurements and crystallographic analyses on structure-H type gas hydrate formed from the CH_4-CO_2-neohexane-water system. *J Phys Chem B*. 2006;110:4583–4588.
31. Wilson LD, Tulk CA, Ripmeester JA. Instrumental techniques for the investigation of methane hydrates: cross-calibrating NMR and Raman spectroscopic data. Paper presented at 4th International Conference on Gas Hydrates, May 19–23, Yokohama, Japan; 2002.
32. Mori YH. Recent Advances in hydrate-based technologies for natural gas storage-a review. *J Chem Ind Eng (China)*. 2003;54:1–17.
33. Thomas S, Dawe RA. Review of ways to transport natural gas energy from countries which do not need the gas for domestic use. *Energy*. 2003;28:1461–1477.
34. Englezos P, Lee JD. Gas hydrates: A cleaner source of energy and opportunity for innovative technologies. *Korean J Chem Eng*. 2005;22:671–681.
35. Lee JD, Susilo R, Englezos P. Kinetics of structure H gas hydrate. *Energy Fuels*. 2005;19:1008–1015.
36. Vysniauskas A, Bishnoi PR. A kinetic-study of methane hydrate formation. *Chem Eng Sci*. 1983;38:1061–1072.
37. Englezos P, Kalogerakis N, Dholabhai PD, Bishnoi PR. Kinetics of formation of methane and ethane gas hydrates. *Chem Eng Sci*. 1987;42:2647–2658.
38. Englezos P, Hall S. Phase equilibrium data on carbon dioxide hydrates in the presence of electrolytes, water soluble polymers and montmorillonite. *Can J Chem Eng*. 1994;72:887–893.

Manuscript received Oct. 16, 2007, revision received Dec. 4, 2007, and final revision received Apr. 24, 2008.